Prognostic and Health Management System for Hydraulic Servoactuators for Helicopters Main and Tail Rotor

Andrea Macaluso[1]

[1] *Politecnico di Torino - Department of Mechanical and Aerospace Engineering, Turin, 10129, Italy*

andrea.macaluso@polito.it

ABSTRACT

The research herein presented continues an initial work on this area performed at Politecnico di Torino in the past years and moves forward in the definition of an effective PHM system for Electro-Hydraulic Servo Actuators (EHSA). PHM of EHSAs is an area only little addressed, but of great interest for the aerospace industry and the air fleet operators. The PHM algorithm consists of three subroutines: the first subroutine extracts a set of relevant features from the data acquired by the sensors during a pre or post flight set of commands and mitigate their dependencies with environmental condition. Fault identification is then performed using mathematical data-driven techniques, three methods are presented: Nominal bands, Percentual error and Euclidean distance. Classification of a single and multiple degradations is performed by the second subroutine with the aid of two dual layer Neural Networks. Finally, the remaining useful life (RUL) is estimated by the third subroutine using a particle filter framework, where the feature evolution model is estimated online. Electro-hydraulic Servo-valves (EHSV) faults are widely addressed with the aid of a nonlinear model and the performance of the PHM algorithm is assessed using relevant metrics.

1. INTRODUCTION

Research activities on PHM systems is an area of great interest for the aerospace industry. In the last decades the development and implementation of such systems have been primarily focused on structures and power drives. Some research work has been reported on PHM for electromechanical flight control, while electrohydraulic servo-actuator for primary flight control systems have been only little addressed so far. Flight control for main and tail rotor are more prone to failure than flight control actuator for fixed wing aircraft, due to the vibrational environment, that leads to a shorter time between overhaul. PHM

technologies aims to contribute towards the transition from scheduled maintenance to Condition Based Maintenance (CBM), improving aircraft dispatchability and reducing maintenance costs.

2. EHSA CONFIGURATION

The EHSA, used as a reference in this research, is a duplex tandem electrohydraulic actuator with a duplex Stability and Control Augmentation System (SCAS). The SCAS consists of two hydraulic actuators, each controlled by an electrohydraulic servo-valve commanded by the Flight Control System. A linear variable differential transformer (LVDT) is used to close the position control loop of the SCAS actuator. Each hydraulic section of the duplex tandem actuator is supplied by a main control valve (MCV). The spool of the MCV is linked to a lever that sums the displacement of the input lever, the SCAS sum lever and the feedback lever. The last one is used to close the position loop of the actuation system. A spherical bearing connects the rod-end of the duplex tandem actuator to the linkage connected to the swashplate.

To enable prognostics a set of non-safety critical sensors is added to the EHSA:

- An additional LVDT measures the displacement of the duplex tandem actuator, this is a standard feature of a Fly-by-Wire EHSA.
- A Differential pressure transducer is used to sense the differential pressure between the two chamber of each section of the duplex actuator.

Moreover, the oil temperature and supply pressure is available at system level in the hydraulic circuit.

2.1. Servo-valve degradation

According to a Failure mode, effects and criticality analysis (FMECA) most common degradations of EHSV are:

- Reduction of the torque of the first stage torque motor.
- Contamination of the first stage filter and nozzles.

- Stiffness variation of the internal feedback spring.
- Increase of the backlash at the mechanical interface between the internal feedback spring and spool.
- Variation of the friction force between spool and sleeve.
- Increase of the radial clearance between spool and sleeve and change of the shape of the corners of the spool lands.

All these faults mode are addressed by the PHM system.

3. MATHEMATICAL MODEL

The system behavior in nominal and degradation conditions is studied with the aid of a high-fidelity mathematical model implemented in Matlab-Simulink. The non-linear physical relations involve physical parameters of each component, that can be modified to inject degradations. The description is herein mainly focused on the SCAS section of the model.

The servo-valve torque motor is modelled using equation presented by Urata (2007), that allows to express the torque as a function of the armature position, misalignment and unequal air-gap thickness. The electromagnetic torque is combined with the dynamic equation of the flapper, connected to the spool by means of the feedback wire. The position of the flapper results in a variation of the differential pressure between the two nozzles, that drives the valve spool. Each parameter of the equations, such as feedback wire stiffness, Coulomb and viscous friction, flow gains and pressure gains can be modified to induce degradation. The EHSV and MCV control flow is function of the spool position, radial clearance, Reynold number and pressure. Oil properties, such as density, viscosity and bulk modulus, are computed using a set of equations that are functions of oil temperature.

Continuity equations describe flows and pressures inside the chamber of the actuator. Coulomb friction depends on the dynamic condition of the actuator and on the geometrical and physical data of the seal, as well as on the pressures in the actuator chambers. Compliance of the linkage is neglected since the load acting on the SCAS is negligible.

LVDTs are modelled including low-pass demodulation filters and analog-to-digital converters, taking into account electrical noise. The mathematical model allows simulating the aerodynamic load acting on the rotor, comprised of the sum of four components: aircraft velocity, atmospheric wind, wind gust and turbulence, implemented using the Dryden model.

4. FEATURES EXTRACTION

Features used in the PHM framework are extracted processing the available signals during a sequence of selected stimuli provided during pre-flight or post-flight by the SCAS (Figure 1) with one hydraulic section engaged.

The command is designed to maximize the number of features related to degradations of the servo-valve (Jacazio, G., Mornacchi, A., & Sorli, M., 2015), but can be used also to investigate degradations of the tandem actuator. The features extracted are listed in Table **1**.
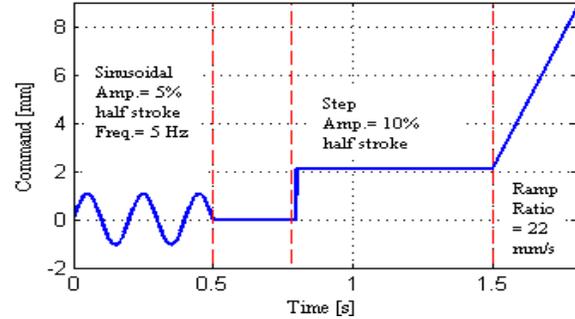

Figure 1: PHM pre/post-flight command

Table 1: Features for EHSV degradation

Command	Position	Current
Sinusoidal	Gain	Min Current
	Phase	Max current
		Mean current
Step	Rise time	Decries time
Ramp	Rate error	Rate current

4.1. Feature correction and performance

The dynamic behavior of the system is strictly related to the environmental conditions, external load and noise. When the aircraft is on ground the aerodynamic load is negligible, on the other hand oil temperature and supply pressure strongly influence the behavior of the system and the value of the features extracted in pre or post-flight. An extensive simulation campaign has been carried out to investigate the sensitivity of the features to oil temperature and supply pressure, without injecting any degradations. Relations that express the features values as a function of these two variable are obtained fitting the set of data, this operation is performed once during the development of the PHM algorithm. Each feature is then corrected to mitigate the effect of temperature and supply pressure:

$$F'_j = F_j(T, P) - f_j(T, P)$$

Where F_j is the *j-th* feature, f_j is the fitted function and F'_j is the corrected feature. The correlation of the features to the oil temperature and supply pressure is calculated as:

$$r_{D,F} = \frac{1}{N-1} \sum_{i=1}^{N} \frac{(Di - \mu_D)(F_i - \mu_F)}{\sigma_D \sigma_F} \qquad (1)$$

Where: μ and σ are the mean and standard deviation, D is one of the variable parameters, and F is the feature. N is the number of samples of each feature and variable, i.e. the number of test performed. The correlation coefficients of some of the current features, before and after correction are

2

listed in Table 2, as expected the corrected features have a smaller correlation with temperature and pressure.

Table 2: correlation of the features with supply pressure and oil temperature before and after correction

Feature	Ps correlation coefficient		Toil correlation coefficient	
	Raw	Corr.	Raw	Corr.
Imax	-0.907	-0.012	-0.987	-0.019
Imean	-0.533	-0.533	-0.984	-0.029

The correlation between the current features after correction and degradation type is then assessed, using equation (1). The correlation between friction, magnetomotive Force (MMF) are listed, as an example, in Table 3. Variation of friction force shows to be the less correlated faults mode with the current features, however it is well correlated with position features: Gain and Phase. Every faults mode have a correlation coefficient above 0.98 with at least two features.

Table 3: correlation of current features with degradations

Degradation	Imax	Imean	Imin	Dec. time	Rate curr.
Frict.	0.921	-0.218	-0.898	0.670	0.040
MMF	0.994	-0.998	0.978	0.980	0.988

5. PHM ALGORITHM

The PHM algorithm consists of three subroutines: Feature extraction and fault identification, using Data-Driven techniques; Fault classification with Neural Network (NN) and prediction of the RUL. The algorithm has been tested using simulation data injecting degradation proportional to the square of flight hours.

5.1. Fault identification

Three different Data-Driven techniques are analyzed to perform fault identification: Nominal bands, Percentual error of the probability density function and Euclidian distance of a reduced set of features found using Principal Component Analysis (PCA).

The Nominal bands methods is discussed in Jacazio et al. (2015). It consists on checking that the feature lays inside a nominal variation range. If an index overcome these limit for three consecutive time a degradation is detected.

The Percentual error method uses an approximation of the probability density function (PDF) of each feature, obtained within a moving window of 50 acquisitions. The actual PDF is compared with a baseline, achieved with 50 acquisitions with the actuator in nominal condition. A degradation is detected when the overlap of the two PDFs is less than a given threshold as shown in **Errore. L'origine riferimento non è stata trovata.**, where a fault detection occurred after 698 flight hours in the presence of an occlusion of 19% and with a detection confidence of 97%. The threshold for detection and the confidence level are defined according to the customer specifications, translated into acceptable

margins for the *type I* and *type II* errors (Mornacchi, A, Vachtsevanos, G., & Jacazio, G , 2015).
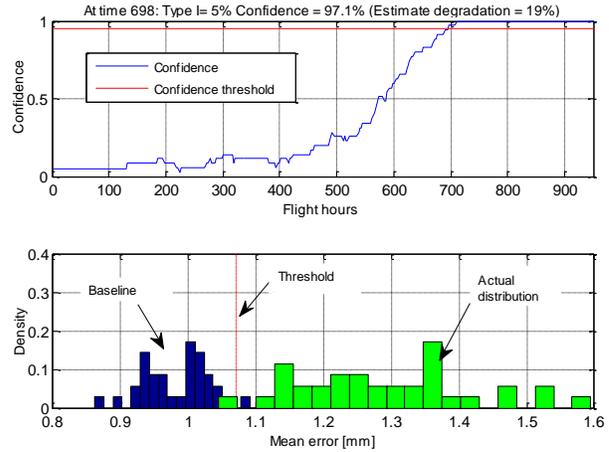

Figure 2: Percentual error, detection of nozzle occlusion

In the third method a set of 50 acquisitions for each feature is acquired, then PCA is used to reduce the features variables from 9 to 2, this two latent variable express more than 98% of the variance of the initial set of data. The probability distribution of the Euclidean Distance (ED) from the mean value is compared with the ED of a set of reference measurements as shown in Figure 3. A degradation is detected when the overlap of the two EDs falls below a threshold, assessed according to customer requirements, as discussed previously.
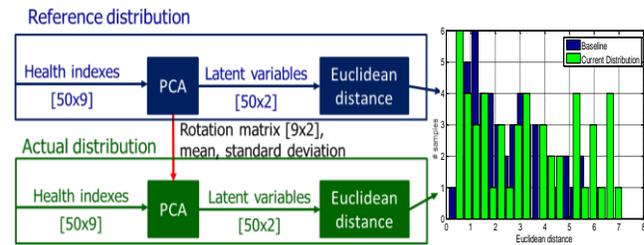

Figure 3: Euclidean distance method

A qualitative comparison of the pros and cons of the three methods is presented in Table 4. An appropriate method can be selected according to the application. In this note the Percentual error method is adopted.

Table 4: Comparison of fault identification techniques

	Pros	Cons
Nominal bands	- Quick identification of a degradation - Does not require to save a set of data	- Difficulties in defining the right tolerance bands - Not self-adapting
Percentual error	- Allows easy comparison with reality - Low computational cost - Autonomously adapting	- Slow identification of degradation
Euclidean distance	- Sensitivity to variation of EHSA characteristics - Autonomously adapting	- High computational cost - Difficulty in defining failure condition

5.2. Fault classification

After a fault has been detected the fault classification routine is activated to classify the fault. In case the degradation has been successfully classified, the algorithm starts to monitor the historical trend of the features to detect and classify a further fault. Classification of the first degradation is performed by a double layer NN that receives the nine features normalized values as input. The NN has 7 outputs one for each degradation class; when the degradation is classified the relative output value is 1 while the others remain 0. A second double layer classifies the presence of further degradation. The second NN has 16 inputs,where the first seven inputs are the indicators of the degradation class and the last nine correspond to the signs of the peaks of the second derivative of the features trend. Both NN were trained using Bayesian regularization backpropagation method, using a random set of 1366 acquisitions for the first degradation and 10 acquisitions for the second NN.

Classification of the first degradation was successful except for 0.31% of the cases, where a high degradation level was present. The classification of the second degradation is more challenging and give a faulty classification in 5.4% of the cases and 1.6% of false alerts.

5.3. RUL prediction

A long-term prediction of the evolution of features is performed using a simplified particle filter framework, with no states estimation.

$$e(t + 1) = e(t) + dt(f_c(t + h) - f_c(t))/h + \omega(t)$$

Where f_c is a non-linear mapping that relate the absolute Percentual error with the flight hours, $e(t)$ is a continuous-values, i.e. the absolute Percentual error, dt is the interval between t and $t+1$, h is delta for the numerical derivative and $\omega(t)$ is noise described like a normal distribution with zero mean. The initial conditions is $e=0$. The actual value of the state $e(t)$ is equal to the last estimation of the prediction step or to a field acquisition, if it is available at the actual time step t. The model that express the evolution of the fault with time, f_c, and its variance, ω, are estimated online, fitting the last 50 samples since fault detection plus 10 samples ahead. In this note only the Percentual errors of Gain is used to calculate the RUL; a moving average filter is applied before the model fitting take place. A frame of 5000 particles are used in the particle filter. Figure 4, shows the output of the RUL prediction.

Performance of the prognostic algorithm is evaluated using the Prognostic horizon, defined as the difference between the current time index i and the end of prediction utilizing data accumulated up to the index i, as proposed by Saxena, Celaya, Balaban, Gobel, Saha B, Saha S, and Schwabacher (2008). The mean Prognostic horizon is equal to 95.3 flight hours.
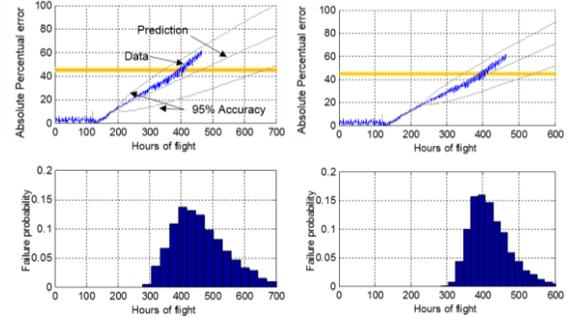

Figure 4: RUL prediction, at the time of fault detection (left) and after 60 hours (right)

6. CONCLUSION

The PHM algorithm is capable to address most common faults mode of the EHSV, accordingly to a FMECA. The algorithm has been applied to a specific EHSA, however it can be applied to a wide range of Fly-by-wire EHSAs or even in a different application domain. Simulations data were used to test the capability of the algorithm. Features correction is a novelty herein presented to improve correlation of features with degradation, resulting in an improvement of the overall performances of the PHM algorithm. Different Data-Driven fault identification methods, based on comparison of acquisition data in nominal versus actual condition, have been presented and evaluated. Prediction of the RUL has been performed, using particle filter, without a previous knowledge of the fault to failure model. Further developments consist on addressing faults of the actuator developing a new set of features from the available sensors signals and testing the algorithm with a dedicated test bench.

REFERENCES

Jacazio, G., Mornacchi, A., & Sorli, M. (2015). Development of a prognostics and health management system for electrohydraulic servoactuators of primary flight controls. *5th International Workshop on Aircraft System Technologies AST2015*, Hamburg, Germany, February 24th – 25th.

Urata, E. (2007). Influence of unequal air-gap thickness in servo valve torque motors. *Proceedings of the Institution of Mechanical Engineers, Part C: Journal of Mechanical Engineering Science.* vol. 221, No. 11

Mornacchi, A, Vachtsevanos, G., & Jacazio, G (2015). Prognostics and Health Management of an Electro-Hydraulic Servo Actuator. *Annual Conference of the Prognostics and Health Management Society 2015,* pp.1,17, October 18th - 24th

Saxena, A., Celaya, J., Balaban, E., Goebel, K., Saha, B., Saha, S., & Schwabacher, M. (2008). Metrics for evaluating performance of prognostic techniques. *International Conference on Prognostics and Health Management,* pp.1,17, October 6th - 9th